PHYSICAL REVIEW D VOLUME 25, NUMBER 1 1 JANUARY 1982

Inclusive π^0 production in 250-GeV/c $\pi^- p$ interactions

R. N. Diamond, S. Hagopian, P. J. Hays, and J. E. Lannutti
Physics Department, Florida State University, Tallahassee, Florida 32306
(Received 20 July 1981)

Neutral-pion production in 250-GeV/c $\pi^- p$ interactions are studied using the Fermilab 15-ft bubble chamber. The mean number of neutral pions produced is 3.54 ± 0.15 per inelastic collision and a fit to a linear dependence on the charged multiplicity gives $\langle n_0 \rangle = 1.30 + 0.56\, n_-$. The π^0 transverse- and longitudinal-momentum distributions are obtained from the inclusive γ-ray data and compared with the distribution obtained from those π^0's which have both decay γ rays converting in the bubble chamber.

I. INTRODUCTION

We present here some results on inclusive neutral-pion production in 250-GeV/c $\pi^- p$ interactions. The experiment was carried out in the Fermilab 15-ft bubble chamber and contains the highest-energy pion-induced bubble-chamber data so far available. A number of experiments at lower energy[1] have established that the mean number of neutral pions is roughly proportional to the number of charged prongs in an event and that the neutral-pion momentum distributions are an average of the charged-pion momentum distributions. Our results confirm and extend these lower-energy trends.

Because of the relatively large size of the Fermilab bubble chamber the γ-ray converison probability is $\sim 14\%$ and enables a statistically large sample of γ-ray conversions to be obtained. As a consequence it is possible to make semi-inclusive measurements of multiplicity and momentum distributions, but that work is left for future publication. Instead we concentrate here on inclusive processes.

II. EXPERIMENTAL DETAILS

The details of the experimental setup and scan procedures have been previously described.[2] The total exposure consisted of 40 337 frames of which 31 770 were acceptable on the basis of beam-track count and picture quality. A total of 22 330 events were found inside a fiducial volume of 2.81 ± 0.02 m; and associated with these events were 12 565 γ rays (G), 2505 neutral strange particles (V), and 12 545 ambiguous two-prong neutral secondaries (A). Subsequent measurements and kinematic fitting of these ambiguous secondaries revealed that $\sim 90\%$ were actually γ-ray conversions. The total number of GA vertices found in the experiment was 25 110. Of the 22 330 events, 9617 had no GA vertex, 5936 had one GA vertex, and 6777 had at least two GA vertices associated with the primary interaction.

As explained in Ref. 2 approximately 15% of the film was double scanned, with discrepancies being resolved by a conflict scan. Because the experiment was an engineering run for the bubble chamber the film quality was poor and several regions of the chamber, such as around the edges of the piston, were at least partially obscured due to formation of dirt and ice on the Scotchlite. As a consequence the scanning efficiency was found to be only $\sim 92\%$ for primary vertices and $\sim 77\%$ for GA vertices.[2]

The original motivation for the experiment was to search for charmed-particle production in events with visible strange-particle decays. This event sample, which is the only data sample to be completely measured, has been published previously.[3] Neglecting a small number of two-, four-, and six-prong events which were completely measured, the measurements basically involved measuring only the GA vertices and the beam track. Thus, in order to compare our results on neutral-pion production with charged-pion results we cannot use the charged-pion momentum distributions in order to simulate the neutral-pion distributions as some other experiments have done.[4] Instead, we derive the neutral-pion momentum distributions from the measured γ-ray distributions.

The strange-particle measurements were made at Fermilab using home-built manually operated measuring machines with $60\times$ magnification and a least count of 1.27 μm on the film and at Florida

State using MicroMetric image plan machines equipped with optically encoded digitizing arms which had a 25× magnification and a least count of 45 μm on the table. Based on a sample of ~2000 noninteracting beam tracks the Fermilab measurements yielded residuals ~11 μm on film, while the Florida State measurements were 50% worse.

The measurements were processed by the HYDRA system of geometrical-reconstruction and kinematic-fitting programs, specifically designed for handling large bubble chambers with fisheye optics and rapidly varying magnetic fields. After completion of remeasurements it was found that ~12% of the events did not fully reconstruct generally because of primary vertex failures.

The following hypotheses were attempted for the two-prong neutral secondary vertices:

$$\gamma+(P \text{ spectator})\rightarrow(P \text{ spectator})+e^+e^- ,$$

$$\gamma\rightarrow e^+e^- ,$$

$$K_S^0\rightarrow\pi^+\pi^- ,$$

$$\Lambda\rightarrow p\pi^- ,$$

$$\bar{\Lambda}\rightarrow\bar{p}\pi^+ ,$$

where the parentheses indicate that the particle was not seen. Both one-constraint fits and three-constraint fits with the neutral particle constrained to come from the primary vertex were attempted. Only 27% of the *GA* vertices fit one and only one hypothesis. In resolving ambiguities we preferred three-constraint fits to one-constraint fits. Ambiguities between different hypotheses of the same constraint class with similar χ^2 confidence levels were broken on the basis of the distribution of momentum (q_T) of the decay products transverse to the neutral particle direction. This distribution, which should peak at 0.0, 0.1, and 0.206 GeV/c for γ, Λ or $\bar{\Lambda}$, and K_S^0, respectively, is plotted in Fig. 1 for a small sample of events which fit the respective hypothesis. We see that 95% of the γ rays have transverse secondary momenta less than 0.025 GeV and that they constitute the largest contamination in the Λ, $\bar{\Lambda}$ and K_S^0 plots. We have therefore selected all neutral two-prong secondaries with $q_T<0.025$ GeV/c as γ rays.

Approximately 70% of the events with at least two *GA* vertices were measured but, since the motivation was to study π^0 production, only ~14% of the single *GA* events were measured. Given a 15% loss rate (12% from geometry failures and 3% for fiducial volume cuts) we are left for further analysis with 4824 events with 11 911 *GA* vertices, 10 238 vertices of which fit some kinematic hypothesis. The 14% of *GA* vertices which give no kinematic fit are mismeasurements of one sort or another and as best we are able to determine constitute an unbiased subset of *GA* vertices.

In order to properly express our results we must associate with each γ ray a weight which incorporates among other things the momentum-dependent γ-ray conversion probability. This conversion weight, obtained from a linear interpolation of conversion length, $l_c(q)$, calculated by Knasel,[5] is given by the expression

$$W_c(l)=1/[e^{-l_{\min}/l_c(q)}-e^{-l_{\max}/l_c(q)}] .$$

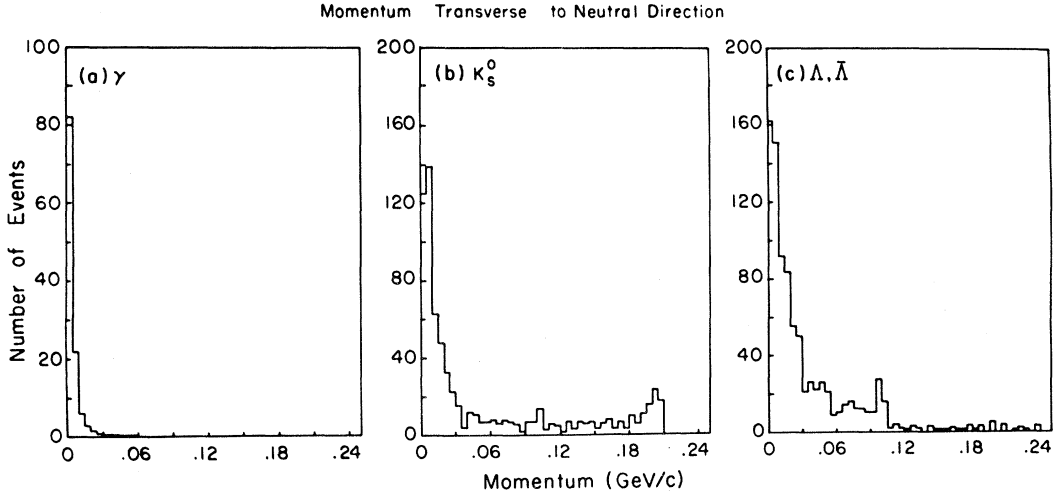

FIG. 1. Measured transverse momentum of a secondary particle with respect to the incident neutral for those vees which fit γ, K_S^0, or (Λ,$\bar{\Lambda}$) hypotheses.

l_{min} and l_{max}, respectively, represent the shortest and farthest distances from the primary vertex that a γ-ray conversion can occur whose measurement will be accepted for further analysis.

l_{max} is determined by the requirement that the γ-ray conversion be at least 45 cm from the wall of the bubble chamber in order to have enough track length for the electron-positron pair so that the γ-ray momentum can be determined with reasonable accuracy. l_{min} is equal to 10 cm. This potential length cut to remove γ-ray conversions close to the primary vertex is made in order to eliminate a possible bias favoring low-momentum conversions, which are more easily identified by our scanners. (The high-momentum conversions are often lost in the forward jet of secondary particles.) We have noted a slight decrease in the number of *GA* vertices between 10 and 35 cm from the primary vertex and, observing no strong momentum bias in this sample, correct for this loss as a function of distance by the weight factor

$$W(x)=1/(a+bx)\ ,$$

where $a = 0.37\pm0.08$ and $b=0.018\pm0.003$ cm^{-1}. An additional weight factor to compensate for geometrical reconstruction and kinematic fitting must also be applied. The distribution of weights for the γ-ray conversions is shown in Fig. 2. The mean weight per γ ray is 26.2 ± 0.11 of which 7.17 ± 0.04 is the mean conversion weight and 3.66 ± 0.09 is due to losses at the various processing stages.

III. RESULTS

Given the weight for each γ ray we can compute the mean π^0 multiplicity. There are 5769 γ rays with a mean weight of 26.2 ± 0.11 giving a total of

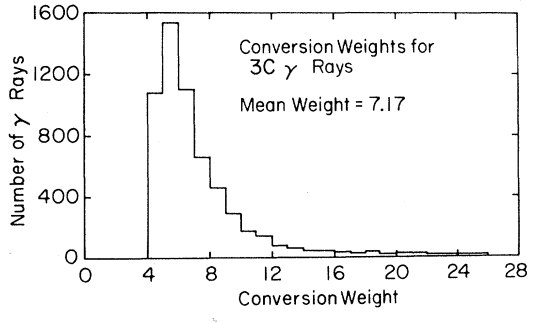

FIG. 2. Distribution of conversion weights for γ rays which yield three-constraint fits.

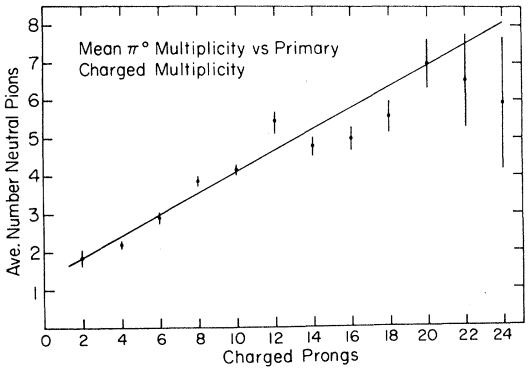

FIG. 3. Mean number of neutral pions per inelastic event as a function of the number of charged pions.

151 351$\pm$645 γ rays produced in the experiment. If γ rays arise solely from π^0 decay the inclusive π^0 cross section is 75.7 ± 3.2 mb, which corresponds to 3.39 ± 0.14 π^0/event or 3.54 ± 0.15 π^0/inelastic collision. The largest contribution to the uncertainty is due to the determination of the scanning efficiencies for γ rays ($\sim$2%). In Fig. 3 we display the mean number of π^0's as a function of the charged particle multiplicity for inelastic collisions. A fit of the form $\langle n^0\rangle = \beta+\alpha n_-$ to the data gives

$$\langle n^0\rangle = 1.3\pm0.2+(0.56\pm0.04)n_-\ .$$

The slope parameter α is consistent with the trend reported by Whitmore[1] indicating an increase with incident momentum. However, it is not clear from the data that the linear fit to $\langle n^0\rangle$ gives an adequate description of the data.

The multi-γ events have been used to calculate the γ-γ invariant-mass distribution which is shown in Fig. 4. A prominent peak in the π^0 mass region (110–150 MeV/c^2) is observed. The curve in Fig. 4 represents a Gaussian-plus-fourth-order-polynomial background. After background subtraction,

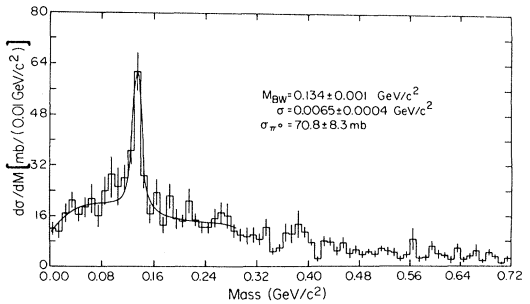

FIG. 4. The γ-γ invariant-mass spectrum. The curve is a fit to a Gaussian-plus-polynomial background.

the excess events correspond to an inclusive π^0 cross section of 70.8 ± 8.3 mb, in good agreement with the cross section obtained from the inclusive γ-ray cross section. If we take the one bin fluctuation in the 0.56—0.57 GeV/c^2 bin of the γ-γ mass plot to be the result of η production, it would correspond to a cross section of 0.45 ± 0.34 mb.

In Fig. 5(a) we display the γ-ray longitudinal-momentum distribution $F(x)$, where

$$F(x)=\frac{2E}{\pi\sqrt{s}}\int\left[\frac{d\sigma}{dp_T{}^2dx}\right]dp_T{}^2 .$$

The γ-ray transverse-momentum distribution $d^2\sigma/dp_T{}^2$ is shown in Fig. 6(a). and the γ-ray rapidity $d\sigma/dy$ is shown in Fig. 7(a). The corresponding distributions for the π^0 are shown in Figs. 5(b), 6(b), and 7(b). We wish to show that these momentum distributions are consistent within statistics and to find a suitable parametrization for the π^0 cross section over the range of kinematic variable for which we have adequate data. Because the number of γ pairs from the same π^0 which are detected in the bubble chamber is quite low (there are some 377 pairs with mass between 0.12 and 0.15 GeV/c in our experiment) the π^0 momentum distributions can be better determined by using the inclusive γ-ray momentum distributions. Kopylov[6] has shown that for any single γ-ray momentum component q_i the corresponding π^0 momentum component p_i is given by

$$N(q_i)=\int_{q_i-M_\pi{}^2/4q_i}^{\infty}\frac{N(p_i)dp_i}{(M_\pi{}^2+p_i{}^2)} .$$

The γ-ray transverse-momentum distribution is related to the π^0 transverse-momentum distribution by the expression

$$N(q_T)-\frac{2}{\pi}q_T\int_{q_T-M_\pi{}^2/4q_t}^{\infty}N(p_T)K(t(p_T),s(q_T))dp_T ,$$

where

$$K(t,s)=2M^{-2}\int_s^t du[(\sinh^2 t-\sinh^2 u)(e^{2u}-e^{2s})]^{-1}$$

and

$$t(p_T)=\ln[(p_T+E)/M_\pi],\quad s(q_T)=\ln(2q_T/M) .$$

As a practical matter following this prescription involves assuming a functional form for the π^0 distributions and adjusting the parameters so as to give the best fit to the γ-ray data. Unfortunately the longitudinal- and transverse-momentum components of the parent π^0's are separated through use of this approach and the π^0 invariant cross section cannot be obtained.

Other authors[4] have taken a suitable combina-

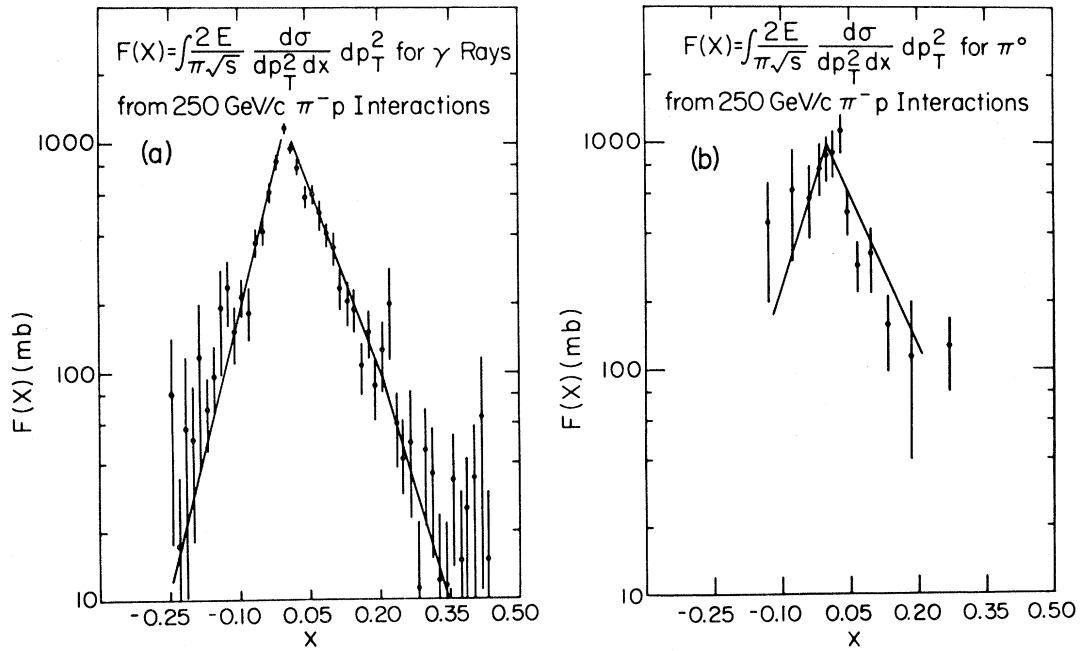

FIG. 5. (a) The distribution $F(x)$ for γ rays. The curve results from a simultaneous fit to this distribution and to the transverse-momentum distribution. (b) The distribution $F(x)$ for π^0s. The curve is obtained from the fit to the inclusive γ-ray data.

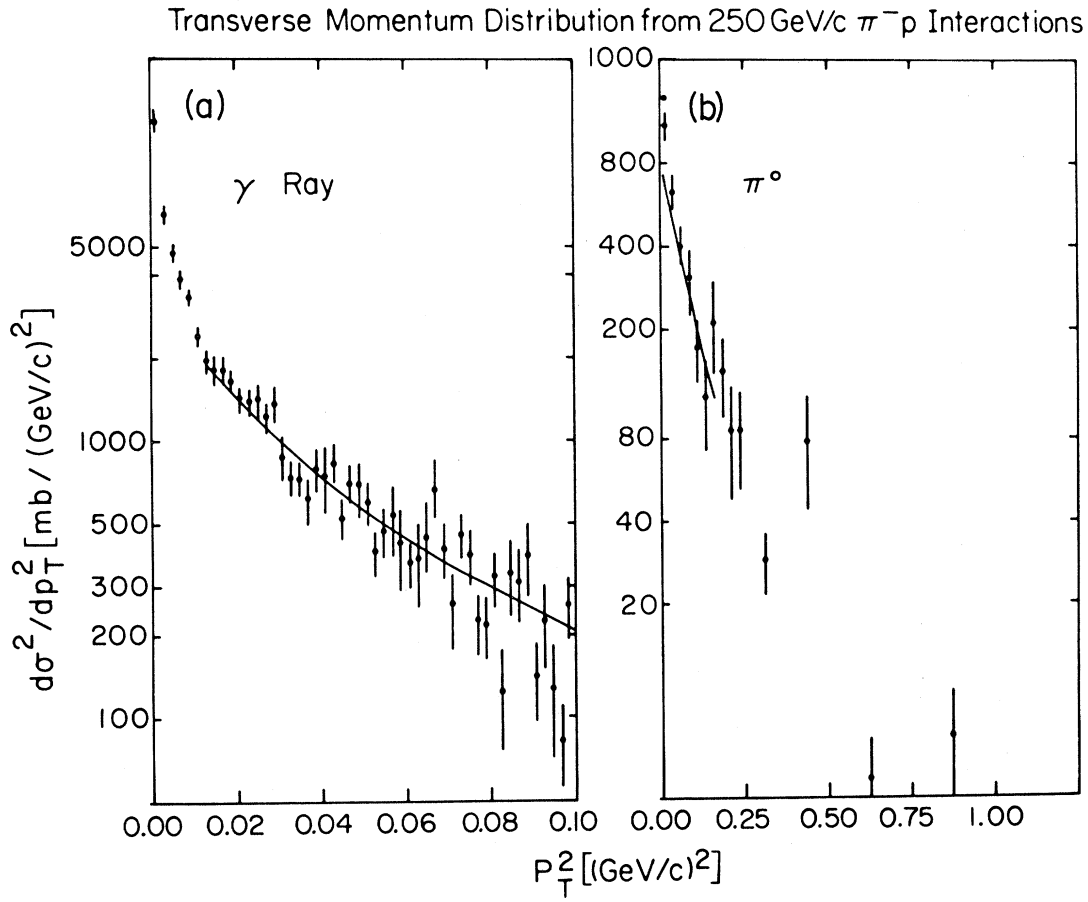

FIG. 6. (a) The γ-ray transverse-momentum distribution. The curve results from a simultaneous fit to this distribution and to the $F(x)$ distribution. (b) The π^0 transverse-momentum distribution. The curve is obtained from the fit to the inclusive γ-ray data.

tion of π^+ and π^- momentum distributions to represent the π^0 production spectrum and show that the observed inclusive γ-ray distributions are consistent with having resulted from the decay of π^0's produced with that spectrum. Because we have not measured the inclusive charged-pion cross sections we cannot adopt this approach.

We choose instead to consider the reaction

$$AB \rightarrow CX \searrow 1,2 ,$$

the invariant cross section for which can be written as

$$\sigma = \int \frac{dS_c}{2\pi} \frac{2\sqrt{s_c}\,\Gamma(c \rightarrow 1,2)}{(s_c - m_c^2)^2 + m_c^2\Gamma^2} \times \mathrm{Tr}(\rho A^*)\sigma_c dp_{\mathrm{LI}}(s_c, p_1, p_2) ,$$

where ρ and A are the production and decay density matrix elements for particle C, and dp_{LI} is the Lorentz-invariant phase-space element. For the $\pi^0 \rightarrow \gamma_1\gamma_2$ decay, $\mathrm{Tr}(\rho A^*)$ is a constant, and taking the narrow-width limit we can write

$$E_{\gamma_1}\frac{d\sigma}{dp_{\gamma_1}^3} = 8\pi \int \left[E_{\pi^0}\frac{d\sigma}{dp_{\pi^0}^3} \right] \frac{d^3p_{\pi^0}}{E_{\pi^0}} \frac{d^3p_2}{4E_2} \frac{\delta^4(p_{\pi^0} - p_1 - p_2)}{(2\pi)^2} = \frac{1}{2\pi} \int E_{\pi^0}\frac{d\sigma}{dp_{\pi^0}^3} \frac{d^3p_{\pi^0}}{E_{\pi^0}E_2} \delta(E_{\pi^0} - E_1 - E_2) .$$

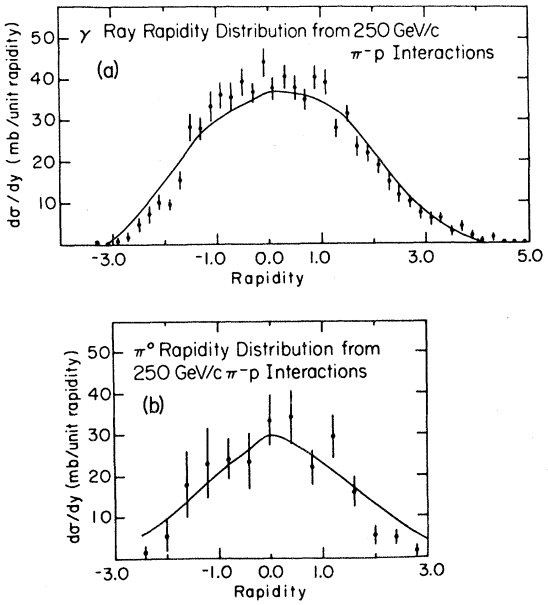

FIG. 7. (a) The γ-ray rapidity distribution. The curve results from a simultaneous fit to the γ-ray $F(x)$ and transverse-momentum distributions. (b) The π^0 rapidity distribution. The curve is obtained from the fit to the inclusive γ-ray data.

If we neglect the mass of the π^0 so that the produced γ rays are collinear with the π^0 then, performing the π^0 angular integration yields

$$E_\gamma \frac{d\sigma}{dp_\gamma{}^3} = 2\int_{2p_\gamma/\sqrt{s}}^{1} \left[E_{\pi^0} \frac{d\sigma}{dp_{\pi^0}{}^3} \right] \frac{d^3z}{z} ,$$

where $z = p_\gamma / p_\pi$. The observed γ-ray transverse- and longitudinal-momentum distributions can be fitted simultaneously to better determine the parameters of the π^0 invariant cross section. Thus given $p_\gamma = (p_{T\gamma}, p_{L\gamma})$ one can find $E_\pi d\sigma / d^3p_\pi (p_{L\gamma}/Z, p_{T\gamma}/Z)$.

We parametrize the π^0 invariant cross section by the form

$$\frac{2E}{\pi\sqrt{s}} \frac{d^3\sigma}{dp_T{}^2 dx} = Ae^{-Bp_T} e^{-Cx} ,$$

where $x = 2p_L^*/s$, p_L^* being the π^0 cm longitudinal momentum. Because the distribution $F(x)$, which is the integral of the invariant cross section, is not symmetric about $x = 0$, we have actually used two parameters C_+ and C_- for the forward and backward dependence. The values of the parameters, obtained by simultaneously fitting the X and p_T distributions, are

$$A = 39.2 \pm 2.1 \times 10^5 \text{ mb/GeV}^2 ,$$

$$B = 8.85 \pm 0.05 \text{ GeV}^{-1} ,$$

$$C_- = 14.8 \pm 0.1 ,$$

$$C_+ = 10.4 \pm 0.4 .$$

The curves resulting from this parametrization are shown in Figs. 5(a) and 6(a). The χ^2/DF is approximately 1. The π^0 distributions obtained from these fits are plotted in Figs. 5(b) and 6(b). Good agreement with our statistically poor π^0 data is evident. Using this same parametrization the γ-ray and π^0 rapidity distributions have been calculated and are plotted in Figs. 7(a) and 7(b). The agreement is reasonable and could be made better by incorporating the γ-ray rapidity distributions in the fit.

We have attempted without much success to use other parametrizations, as, for example, have been suggested by Taylor *et al.*,[7] for the π^0 invariant cross section. Most of these parametrizations apply to regions of transverse and longitudinal momentum higher than those in which the bulk of our bubble-chamber data occurs. The large amount of data at low p_T and low X may result from π^0 production via the decay of heavier resonances such as ρ, f^0, etc.. In Ref. 2 we reported on attempts to fit the charged-particle multiplicity distributions using two component models with a low-multiplicity diffractive component and a higher-multiplicity nondiffractive (cluster) component. Clusters with ~ 2 charged particles were necessary to account for the charged multiplicity distribution. We would expect a similar situation for neutral-pion production.

The actual functional form used in the fitting procedure has no particular significance. Other forms may fit as well. The good agreement between the π^0 distributions obtained from the inclusive γ-ray data and the measured π^0 distributions demonstrate that in the bubble chamber the neutral-pion differential cross sections can be obtained directly from the inclusive γ-ray data. What is needed is a higher-statistics experiment in the low-X, low-p_T kinematic region in order to better determine the π^0 differential cross section.

ACKNOWLEDGMENTS

We would like to acknowledge the help we received from the Fermilab bubble-chamber group, in particular F. R. Huson, J. P. Berge, D. Bogert,

R. Hanft, R. Harris, S. Kahn, and W. Smart during the early stages of the experiment. The scanning and measuring crews at Fermilab and Florida State are acknowledged for their work with difficult film. We also wish to thank J. F. Owens for valuable discussions of the fitting procedure. This research was supported in part by the U.S. Department of Energy.

---

[1]J. Whitmore, Phys. Rep. 10C, 302 (1974).
[2]P. J. Hays *et al.*, Phys. Rev. D 23, 20 (1981).
[3]D. Bogert *et al.*, Phys. Rev. D 16, 2098 (1977).
[4]N. N. Biswas *et al.*, Nucl. Phys. B167, 41 (1980).
[5]T. M. Knasel, DESY Report No. 70/3, 1970 (unpublished).
[6]G. I. Kopylov, Nucl. Phys. B52, 126 (1971).
[7]F. E. Taylor *et al.*, Phys. Rev. D 14, 1217 (1976).